phys. stat. sol. (a) **178**, 277 (2000)

Subject classification: 71.35.Cc; 73.20.Dx; 78.47.+p; S7.12

# Excitonic and Biexcitonic States in Semiconductor Quantum Dots

U. HOHENESTER[1]) and E. MOLINARI

*Istituto Nazionale per la Fisica della Materia (INFM) and Dipartimento di Fisica, Università di Modena e Reggio Emilia, Via Campi 213/A, I-41100 Modena, Italy*

(Received August 30, 1999)

We analyze excitonic and biexcitonic effects in the coherent optical spectra of semiconductor quantum dots using a density-matrix approach, that explicitly accounts for exciton–exciton interactions. A consistent description of additional peaks appearing at higher photoexcitation density is given.

In semiconductor quantum dots (QDs) photogenerated electron–hole pairs remain bound because of the strong three-dimensional quantum confinement. Thus, in the optical spectra of QDs a strong enhancement of excitonic effects is expected as compared to semiconductor systems of higher dimensionality, where carrier complexes can break up into spatially separated constituents. Indeed, clear experimental evidence of pronounced Coulombic few-particle effects was recently reported in the nonlinear optical spectra of single QDs [1 to 5]: additional emission peaks appear with increasing excitation density, which then supersede the original lines when the density is further increased.

Using a density-matrix approach at the level of two-particle correlations, in this paper we present a theoretical study of the excitonic properties of semiconductor QDs. We analyze single-exciton effects in the linear magneto-optical spectra, and we compute the nonlinear optical response by use of a time dependent pump–probe setup. Our results allow us to discuss the nature of additional peaks appearing in the nonlinear optical spectra.

Within a density-matrix approach, at each instant of time the carrier system is characterized by its one-particle density matrix and its higher-order correlation functions. The time evolution of these dynamic variables is obtained from the Liouville-von Neumann equation, which couples through the Coulomb potential all higher-order correlations. Thus, as a central approximation of any density-matrix approach one has – based on physical intuition – to truncate this hierarchy of equations. A particularly transparent truncation scheme follows for the coherent optical response, i.e., the optical response in absence of dephasing processes [6]. Classifying the coherent optical response in powers of the electric field of the laser light, it turns out that: 1. the linear optical response is described by the interband polarization $p$, which accounts for macroscopic phase coherence of electron–hole pairs introduced by the coherent laser field; 2. for the third-order optical response only one additional quantity $b$, which accounts for biexcitonic effects, is required [6, 7].

[1]) Corresponding author; Fax: +39 059 367488; e-mail: hohenester@unimo.it

In our calculations for the QD, we start from the single-particle wavefunctions, $\phi$, and energies, $\epsilon$, derived by solving the single-particle Schrödinger equation within the envelope-function and effective-mass approximations, by means of a plane-wave expansion with periodic boundary conditions [8]. For the linear optical response we obtain the excitonic wavefunctions $\Psi^x_{\mu\nu}$ and energies $E_x$, which describe one interacting electron–hole pair confined in the QD, from the solutions of the excitonic eigenvalue problem [8, 9]

$$(\epsilon^{\mathrm{e}}_{\mu} + \varepsilon^{\mathrm{h}}_{\nu})\, \Psi^x_{\mu\nu} - \sum_{\mu'\nu'} V^{\mathrm{eh}}_{\mu\mu',\nu\nu'} \Psi^x_{\mu'\nu'} = E_x \Psi^x_{\mu\nu}\,, \tag{1}$$

through an expansion in terms of single-particle states for electrons (holes) which are labeled by $\mu(\nu)$. Here, $V^{\mathrm{eh}}_{\mu\mu',\nu\nu'}$ are the electron–hole Coulomb matrix elements. Expanding the interband polarizations $p$ and the biexcitonic transitions $b$ in terms of $\Psi^x$, we then obtain for the third-order optical response the following set of dynamic equations [6, 7]:

$$\dot{ip}_x = E_x p_x + \sum_{x',\bar{x},\bar{x}'} \bar{V}_{xx',\bar{x}\bar{x}'} p^*_{x'} (p_{\bar{x}} p_{\bar{x}'} + b_{\bar{x}\bar{x}'}) - \mathcal{E}\left( M_x - \sum_{\bar{x}\bar{x}'} \bar{M}_{x,\bar{x}\bar{x}'} p^*_{\bar{x}} p_{\bar{x}'} \right), \tag{2a}$$

$$\dot{ib}_{xx'} = (E_x + E_{x'})\, b_{xx'} + \sum_{\bar{x},\bar{x}'} \bar{V}_{xx',\bar{x}\bar{x}'} (p_{\bar{x}} p_{\bar{x}'} + b_{\bar{x}\bar{x}'})\,, \tag{2b}$$

with $\mathcal{E}$ the electric field of the laser light (treated within the rotating-wave approximation); $M$ and $\bar{M}$ the optical matrix elements (treated within the dipole approximation): within the envelope-function approximation, these optical interband matrix elements are of the form $\propto \int \mathrm{d}\mathbf{r}\, \phi^{\nu_h}_{\mathrm{h}}(\mathbf{r})\, \phi^{\nu_e}_{\mathrm{e}}(\mathbf{r})$ [8]. For the coupling of excitons with opposite spin orientation, the exciton–exciton Coulomb matrix elements $\bar{V}_{xx',\bar{x}\bar{x}'}$ in Eq. (2) account for a conventional dipole–dipole interaction,

$$\bar{V}_{xx',\bar{x}\bar{x}'} = \int \mathrm{d}\mathbf{r}\, \mathrm{d}\mathbf{r}' \frac{\mu_{xx'}(\mathbf{r})\, \mu_{\bar{x}\bar{x}'}(\mathbf{r}')}{\kappa_0 |\mathbf{r} - \mathbf{r}'|} \tag{3}$$

with $\kappa_0$ the static dielectric constant and $\mu_{xx'}$ the dipole moment corresponding to the excitonic transitions from $x'$ to $x$. For the coupling of excitons with parallel spin orientation, in addition a proper antisymmetrization with respect to the two electron (hole) coordinates in Eq. (3) is performed [7].

We finally analyze the various contributions to Eq. (2) in slightly more detail: first, the excitonic Coulomb interactions in Eq. (2a) consist of a mean-field contribution $\propto p^3$, and of a coupling between $p$ and $b$; as will be shown further below, this coupling is responsible for the appearance of additional peaks in the nonlinear optical spectra. The coupling between $p$ and the light field is described by $M$ where $\bar{M}p^*p$ accounts for phase-filling corrections due to photogenerated electron–hole pairs. In Eq. (2b) the term $\bar{V}p^2$ acts as a source term which describes how biexcitons build up in the presence of photogenerated carriers. Finally, $\bar{V}b$ couples the different biexcitonic transitions and leads to a renormalization of the biexcitonic spectrum (i.e., "bound" biexcitons versus scattering states).

In this paper we consider a prototype QD confinement potential which is parabolic in the $(x, y)$-plane and box-like along $z$. The confinement energies due to the in-plane

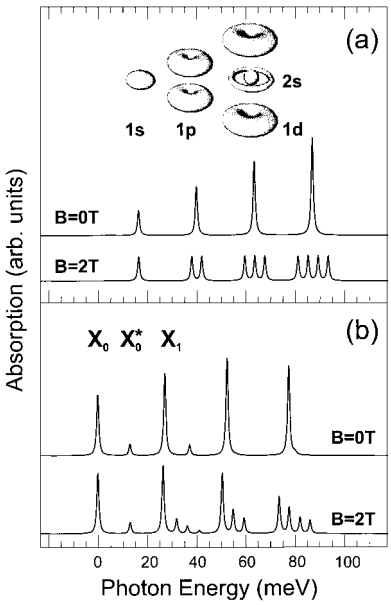


Fig. 1. Optical absorption spectra for a parabolic QD and for two different magnetic fields; a) b) electron–hole Coulomb interaction neglected (included). Photon energy zero is given by the energy of the groundstate exciton $X_0$. The inset sketches the six energetically lowest single-particle states

parabolic potential are $\omega_0^{\mathrm{e}} = 20$ meV for electrons and $\omega_0^{\mathrm{h}} = 3.5$ meV for holes (with this choice, electron and hole wavefunctions have the same lateral extension; we use material parameters for GaAs), and the quantum-well confinement along $z$ is such that the intersubband splittings are much larger than $\omega_0^{\mathrm{e,h}}$. The inset of Fig. 1a sketches the wavefunctions of the six energetically lowest single-particle states. Since in cylindrical coordinates $(r, \phi, z)$ the single-particle wavefunctions factorize, they can be characterized by the quantum numbers $(n, m, n_z)$ [10]; for convenience, we denote the states $(n, |m|) = (1,0)$, $(1,1)$, $(1,2)$, and $(2,1)$ with 1s, 1p, 1d, and 2s, respectively. Finally, because electron and hole wavefunctions have the same lateral extension and owing to wavefunction orthogonality, optical transitions are only allowed between electron and hole states of corresponding quantum numbers $(n, m)$.

Fig. 1a (Fig. 1b) shows optical absorption spectra which are computed without (with) electron–hole Coulomb interaction. In Fig. 1a, at zero magnetic field ($B = 0$) the energy splitting of the absorption peaks is given by the sum of the confinement energies for electrons and holes, and the height of each peak reflects the degeneracy of the respective single-particle states; in the presence of a small magnetic field, transitions with nonzero angular momentum $m$ undergo a Zeeman splitting and the degeneracy of all shells is lifted [11]. A closer inspection of the differences between Fig. 1a and b indicates that Coulomb interactions are important for a quantitative description of the spectra and cannot be neglected in the theory. Three pronounced effects are present: 1. a redshift of the transitions energies of $\sim 10$ meV (exciton binding energy) due to the attractive Coulomb interaction between electrons and holes; 2. the appearance of additional peaks; e.g., peak $X_0^*$ is caused by the electron–hole Coulomb coupling in Eq. (1) between the optically allowed single-particle transition $(\mu, \nu) = (1s, 1s)$ and the optically forbidden one (1s, 2s); more specifically, we find that the groundstate exciton $X_0$ has a strong (1s, 1s) character with an only small (1s, 2s) contribution, whereas the exciton $X_0^*$ has a large component of the "dark" (1s, 2s) transition and only its small (1s, 1s) contribution couples $X_0^*$ to the light field; 3. for nonzero magnetic field a transfer of oscillator strength between two peaks with small energetic separation caused by the coupling of two optically allowed transitions (e.g., (1p, 1p)). Fig. 2 shows a fan plot of the magneto-optical absorption peak. One clearly observes the Zeeman splitting of the excitonic transitions with p and d character, and at higher magnetic fields a pronounced diamagnetic shift of all transitions. Morever, whenever two excitonic transitions are close in

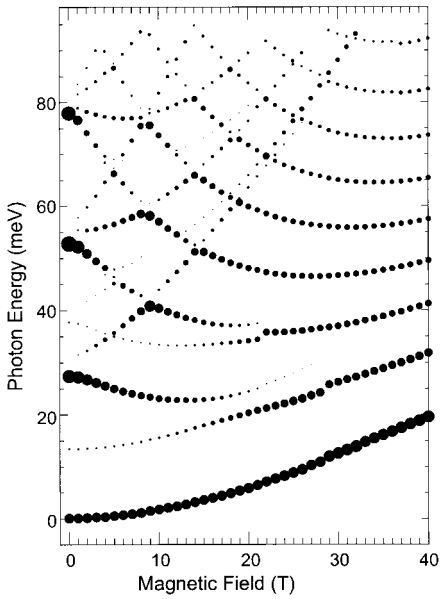


Fig. 2. Optical absorption spectra for different magnetic fields. The size of the dots corresponds to the height of the respective absorption peaks

energy most of the oscillator strength of the energetically higher transition is transferred to the energetically lower one. Finally, at the highest magnetic fields Landau levels are formed.

The nonlinear coherent optical response is analyzed in the time domain in terms of a spin selective pump–probe setup: first, electron–hole pairs with a given spin orientation are generated by a strong pump pulse, where the density and shape of the photogenerated carrier distribution is tuned by the strength of the electric field and the photon energy of the laser. The response of the previously photoexcited system is then investigated by a very weak and short probe pulse (10 fs, for spectral broadness); we directly compute the nonlinear optical response by Fourier-transforming the induced polarization of the probe pulse [8].[2])

Fig. 3a shows the nonlinear absorption spectra as computed from the solutions of Eq. (2) for a pump pulse which creates excitons $X_0$ with spin orientation $\sigma_+$ (with an exciton density $N_{X_0} \sim 0.3$), and for a probe pulse with spin orientation $\sigma_+$ ($\sigma_-$ in Fig. 3b); note that for spin-parallel pumping and probing the nonlinear optical response at zero photon energy strongly depends on the detuning of the probe pulse with respect to the exciton energy $E_{X_0}$. A comparison of the nonlinear optical spectra with the excitonic absorption spectrum of Fig. 1b shows that additional peaks (e.g., $B_0$) appear when the QD is initially populated with photogenerated carriers. We find that the height of these additional peaks increases with increasing electric field of the pump pulse, whereas the excitonic peaks start to quench [13]. These additional spectral features are thus attributed to biexcitonic states.

From Fig. 3 we observe that the energy renormalization of biexcitonic states ranges from $\sim 1$ meV for $B_0$ to $\sim 5$ meV for the biexcitonic resonances $B_1^*$ and $B_3^*$ (see also inset of Fig. 3). To gain further insight into the mechanism responsible for such energy renormalization, in the following we analyze Eq. (2b) in slightly more detail; for conceptual clarity, we only consider biexcitonic states consisting of excitons with opposite spin orientation. First, we note that within our present framework of Eq. (2) the term $\bar{V}b$ is responsible for the renormalization of the biexcitonic spectrum. In analogy to the excitonic eigenvalue problem of Eq. (1), the biexcitonic wavefunctions $\bar{\Psi}^{\lambda}_{xx'}$ and energies $\bar{E}_{\lambda}$, which describe two interacting excitons confined in the QD, are obtained by

[2]) In the calculation of the Fourier-transform of the induced polarization we add a small dephasing rate of 0.2 meV.

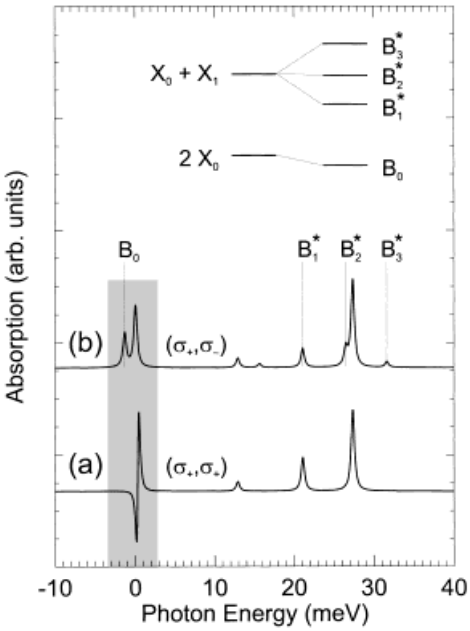


Fig. 3. (a) Nonlinear optical absorption spectra for the spin-parallel pump–probe setup as described in the text; the pump pulse creates excitons at the spectral position $X_0$ (shaded area); (b) Same as (a) but for spin-antiparallel pump–probe setup. The inset sketches the energy renormalization of the biexcitonic states

direct diagonalization from a similar equation:

$$(E_x + E_{x'})\,\bar{\Psi}^{\lambda}_{xx'} + \sum_{\bar{x}\bar{x}'} \bar{V}_{xx',\bar{x}\bar{x}'}\,\bar{\Psi}^{\lambda}_{\bar{x}\bar{x}'} = \bar{E}_{\lambda}\bar{\Psi}^{\lambda}_{xx'}\,. \tag{4}$$

An inspection of $\bar{\Psi}^{\lambda}_{xx'}$ shows that $B_0$ predominantly consists of two excitons $X_0$ with opposite spin orientation. Because of the dipole–dipole character of the exciton–exciton interaction $\bar{V}$ (Eq. (3)), the binding energy of $B_0$ depends on the dipole moment $\mu_{X_0X_0}$; apparently, not the strong (1s, 1s) component of $X_0$ but only its small (1s, 2s) part contributes to $\mu_{X_0X_0}$. In contrast, we find for the wavefunctions of the biexcitonic resonances B* two large contributions: the first one is from the optically allowed excitons $X_0$ and $X_1$; the second one consists of the two "dark" excitons (1s, 1p) and (1p, 1s), which – because of the corresponding strong asymmetry between electron and hole density – give rise to a large dipole moment and, thus, to a larger energy renormalization. Fig. 4 shows the dipole moment $\mu_{xx'}$ for these three excitonic transitions. On a more qualitative level, we interpret our results as follows: since biexcitonic energy renormalization depends on the degree to which excitons can accomodate themselves in presence of other excitons, we expect a smaller renormalization for spatially strongly localized excitons or for exci-

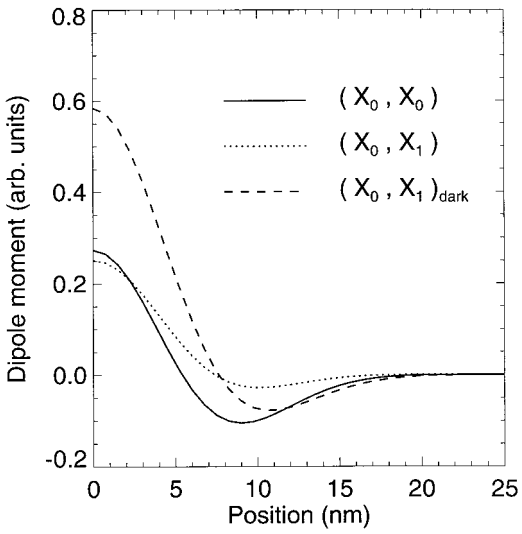


Fig. 4. Dipole moments for different excitonic transitions. $(X_0, X_1)_{dark}$ denotes the coupling between the "dark" (1s, 1p) and (1p, 1s) excitons

tons in filled shells, and a larger renormalization for spatially more extended excitons and for excitons in open shells.

We finally discuss the experimental results that have recently become available from luminescence spectroscopy of single QDs as a function of photoexcitation intensity. Although we shall not attempt a quantitative comparison with our data, from Fig. 3 one immediately observes that our calculations reproduce very well the main experimental trends concerning the appearance of additional lines, as well as their spectral positions. The results of our calculations thus further support the conclusion that interactions of few carriers within a single QD can give rise to a number of additional peaks in the optical spectra [1 to 5].

In conclusion, we have presented a density-matrix approach for the description of photoexcited semiconductor QDs. We have analyzed the magneto-optical properties of a parabolic QD, and we have shown that few-particle interactions play an important role in the appearance of additional lines with increasing pumping density. Finally, we have analyzed their nature within the framework of excitonic interaction processes and of biexcitonic wavefunctions.

***Acknowledgements*** We gratefully acknowledge a number of helpful discussions with Fausto Rossi. This work was supported in part by the EC under the TMR Network "Ultrafast Quantum Optoelectronics". U. H. acknowledges support by the EC through a TMR Marie Curie Grant.

## References

[1] J. MOTOHISA, J. J. BAUMBERG, A. P. HEBERLE, and J. ALLAM, Solid State Electronics **42**, 1335 (1998).
[2] L. LANDIN, M. S. MILLER, M. E. PISTOL, C. E. PRYOR, and L. SAMUELSON, Science **280**, 262 (1998).
[3] E. DEKEL, D. GERSHONI, E. EHRENFREUND, D. SPEKTOR, J. M. GARCIA, and M. PETROFF, Phys. Rev. Lett. **80**, 4991 (1998).
[4] F. VOUILLEZ, D. Y. OBERLI, F. LELARGE, B. DWIR, and E. KAPON, Solid State Commun. **108**, 945 (1998).
[5] F. FINDEIS, A. ZRENNER, M. MARKMANN, G. BÖHM, and G. ABSTREITER, Proc. 9th Internat. Conf. Modulated Semiconductor Structures (MSS9), to be published in Physica E.
[6] V. M. AXT and A. STAHL, Z. Phys. B **93**, 195, 205 (1994).
[7] V. M. AXT and S. MUKAMEL, Rev. Mod. Phys. **70**, 145 (1998).
[8] F. ROSSI and E. MOLINARI, Phys. Rev. Lett. **76**, 3642 (1996); Phys. Rev. B **53**, 16462 (1996).
[9] H. HAUG and S. W. KOCH, Quantum Theory of the Optical and Electronic Properties of Semiconductors, World Scientific Publ. Co., Singapore 1993.
[10] L. JACAK, P. HAWRYLAK, and A. WOJS, Quantum Dots, Springer-Verlag, Berlin 1998.
[11] R. RINALDI, P. V. GIUGNO, R. CINGOLANI, H. LIPSANEN, M. SOPANEN, J. TULKKI, and J. AHOPELTO, Phys. Rev. Lett. **77**, 342 (1996); Phys. Rev. B **57**, 9763 (1998).
[12] U. HOHENESTER, F. ROSSI, and E. MOLINARI, Solid State Commun. **111**, 187 (1999).